Thin Solid Films 518 (2010) 6264–6267

Contents lists available at ScienceDirect

Thin Solid Films

journal homepage: www.elsevier.com/locate/tsf

Development of a hybrid inverter through integration of organic and inorganic thin film transistors

Jung-Ho Park [a], Jae-Hong Kwon [a], Seongpil Chang [a], Han Seo [a,b], Byung-Hyun Choi [b], Mi-Jung Ji [b], Jinnil Choi [a], James Jungho Pak [a], Byeong-Kwon Ju [c,*]

[a] Display and Nanosystem Laboratory, College of Engineering, Korea University, Republic of Korea
[b] Electronic Materials Lab., Korea Institute of Ceramic ENG & TECH, Republic of Korea
[c] School of Electrical Engineering, College of Engineering, Korea University, Republic of Korea

ARTICLE INFO

Available online 8 April 2010

Keywords:
Thin film transistor
Inverter
Hybrid
ZnO
Pentacene

ABSTRACT

In this paper, complementary thin-film transistor (TFT) inverter is fabricated with organic–inorganic hybrid channels. By adopting *p*-channel pentacene and *n*-channel ZnO, we have fabricated a device of hybrid complementary TFT inverter by using same electrode in organic–inorganic hybrid channels. To be accomplished Ohmic-contact in organic–inorganic hybrid channels, we adapted to *n*-channel staggered TFT and *p*-channel coplanar TFT. In results, a hybrid inverter built through integration of organic and inorganic TFT shows that the typical inverter response to stage switching is clearly observed between 0 and 40 V, for both input directions, displaying a high voltage gain — $(dV_{OUT}/dV_{IN})>16$.

1. Introduction

ZnO-based TFT and pentacene-based TFT have been the focus of much research over the last few years for their potential as new representatives of oxide TFT (OxTFT) and organic TFT (OTFT), respectively, which may replace conventional amorphous-Si TFTs [1–3]. Because of high temperature fabrication process and invisible substrate, Si-based TFTs in implementation of flexible and transparent display cannot be adapted. For example ZnO TFTs fabricated at room temperature [4,5]. Currently available complementary TFT (CTFT) inverter is mostly composed of OTFT or OxTFT [6–8]. Generally, complementary inverter is made through integration of *n*-type device and *p*-type device. Especially, both of *p*-channel TFT and *n*-channel TFT have similar performances to exhibit good performance. However, the field effect mobility (μ_{FE}) of *n*-channel OTFT is generally lower than that of *p*-channel counterpart. Contrary, the μ_{FE} of *n*-channel OxTFT is higher than that of *p*-channel counterpart [4,9,10]. *n*-type OxTFT have large electron mobilities because their electron transport paths, i.e., the conduction band minima are made mainly of spatially spread *s* orbitals of metal cations [11]. Moreover *n*-channel organics are generally known to be more susceptible to atmospheric decay than *p*-channel ones (for example, pentacene is known to be quite stable in air as a *p* channel) [12–15]. For this reason, in the last few years work, the hybrid CTFT inverter with *n*-channel ZnO and *p*-channel pentacene have been investigated [16]. However, the hole-transporting and electron-transporting thin-film transistors are integrated in the same device architecture in order to enable complementary circuit technologies, giving one of the most powerful method to enhance the speed and reliability of electronic circuits [17–19]. Other critical difficulties include how to control the threshold voltage (V_T) and how to drive the TFTs at low-voltage, for instance that of the load-TFT in depletion-load-type inverter. Therefore, this research proposes, an appropriate methodology to control the V_T of inorganic and organic TFTs. As reported in the research to date, hybrid inverters have used different source/drain (S/D) electrodes for *n*-channel and *p*-channel devices, respectively [6–8]. Because *n*-channel and *p*-channel materials have different work functions, the same S/D electrode cannot satisfied the Ohmic contact with organic–inorganic hybrid channels at the same time. This problem leads to high process cost, more than that of the two step fabrication process. In order to solve these problems, a structure of CTFT inverter is modified, consisting of staggered ZnO TFT as the *n*-channel device and coplanar pentacene TFT as the *p*-channel device structure [20,21]. By applying a staggered and coplanar structure, despite using the same channel, the Ohmic is achieved between the electrodes and two channels. In this work, the CTFT inverter use same electrode in the oxide-inorganic hybrid channels, different channels length and thickness. Finally, a maximum voltage gain of ~16 is achieved at V_{in} of 20 V.

2. Experimental

The silicon wafer with SiO_2 of 300 nm thickness is used as a substrate. In order to use ZnO as the active channel layer, the background electron concentration of the ZnO thin film must be

* Corresponding author. Tel.: +82 2 3290 3237; fax: +82 2 3290 3791.
E-mail address: bkju@korea.ac.kr (B.-K. Ju).

0040-6090/$ – see front matter © 2010 Elsevier B.V. All rights reserved.
doi:10.1016/j.tsf.2010.03.141

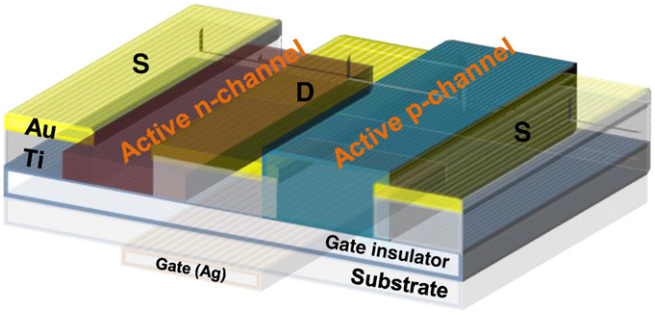

Fig. 1. Schematics diagrams of the hybrid thin film transistor inverter.

reduced [22]. This paper attempts to achieve this by optimizing the deposition conditions and ZnO thin films with 70 nm thickness are deposited on silicon wafer by using rf-magnetron sputtering. A 2-inch diameter ZnO ceramic target is used and the sputtering chamber is evacuated so that the base pressure falls to below 4×10^{-6} Torr. Then, an ultra high purity argon and oxygen gas mixture is injected into the chamber using a mass flow controller (MFC) with the gas mixing ratio of $O_2/Ar+O_2$ being changed from 0 to 20%, and the working pressure maintained at 5×10^{-3} Torr. The active layer is deposited by sputtering without intentional heating in a mixture of argon and oxygen. The distance between the substrate and the target is 8 cm, and the rf power is 100 W. In order to define the active layer, lift-off method is used. A substrate holder is rotated at 12 rpm to ensure uniformity of the deposited thin films. Subsequently, titanium (Ti) and gold (Au) S/D electrodes are sequentially deposited by e-beam/thermal evaporation by loading to another chamber by hand using tweezer and finally, a 90 nm thick pentacene active layer is deposited at a deposition rate of 0.3 Å/s, under a base pressure of 1×10^{-6} Torr using a shadow mask. The film thicknesses are measured using the α-step. The structure properties of the films are measured using X-ray diffraction (XRD) measurements with Cu-Kα radiation. The current–voltage (I–V) characteristics of these TFTs are measured by semiconductor parameter analyzer characterization systems in a dark box at room temperature.

3. Results and discussion

Fig. 1 shows the schematic cross section of the proposed transparent CTFT inverter with the *n*-channel staggered ZnO TFTs and the *p*-channel coplanar pentacene TFT. The reason for the different structures is because suitable S/D electrode material to achieve Ohmic contact in organic–inorganic hybrid channels at the same time. Therefore, the channel should be used in accordance with the other electrode in the CTFT used as the channel. The semiconductor process is required more than twice, and this leads to increased fabrication

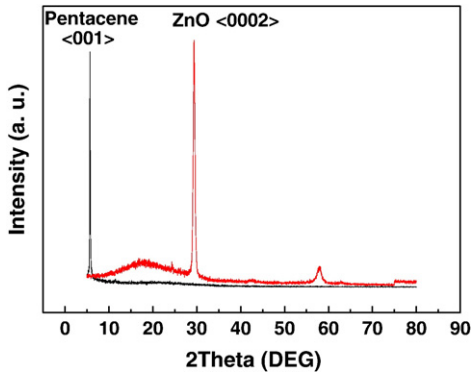

Fig. 2. XRD spectrum of ZnO and pentacene films.

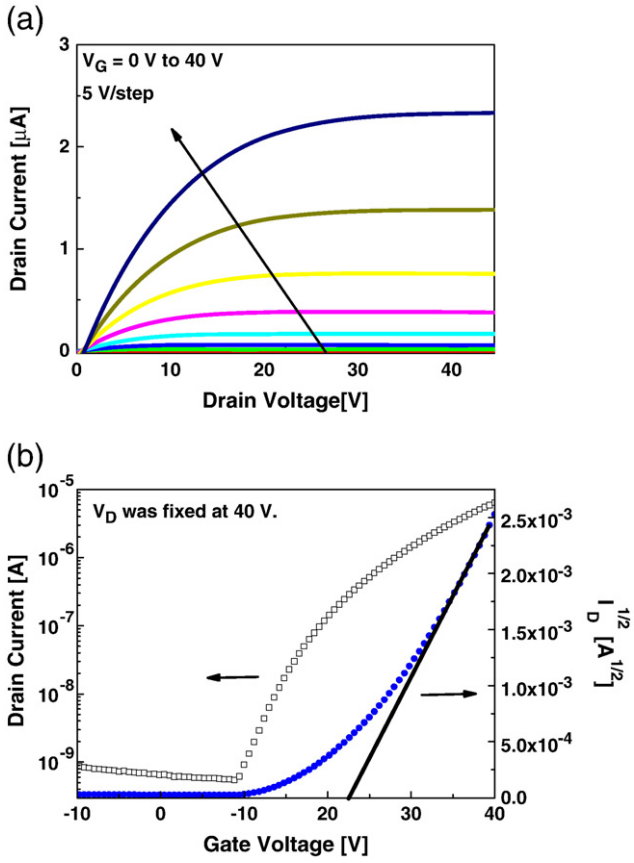

Fig. 3. Electrical properties of ZnO-channel TFT (a) Drain current–drain voltage (I_D–V_D) output curves, (b) transfer curves obtained at a drain bias of 40 V.

cost and complexity. In order to simplify the process, conventional Ti/Au contacts are used; work function of the bottom Ti electrode is 4.09 eV. So, the active ZnO accomplished Ohmic contact in the adapted staggered structure and work function of the upper Au electrode is 4.58 eV. Therefore, the active pentacene achieved Ohmic contact in the adapted coplanar structure. As a result, the S/D electrodes which made once the vacuum deposition process accomplishes Ohmic contact in the *n*-channel ZnO and the *p*-channel pentacene with different bandgap, simultaneously. This is enabling to low cost and a simplified process to be used; in addition, in order for the CTFT inverter to be of good quality, the device property of the *n*-type TFT and the *p*-type TFT should have similar V_T, properties of I_{ON-OFF} and mobilities. Therefore, if the CTFT inverter can be produced a good quality device, *n*-type TFT and *p*-type TFT could be produced with similar electrical characteristics. However, in the published research, OxTFTs are better than OTFT in term of the electronic properties of oxide and organic TFT devices. As a solution, we fabricate the each TFT device with similarly performance of V_T, I_{ON-OFF}, and mobility, how can change channel length and active layer thickness. Fig. 2 shows the X-ray diffraction at the *n*-channel active layer ZnO and *p*-channel active layer pentacene. It is confirmed that the ZnO and pentacene thin films are preferred orientations of (002), and (001), respectively [23,24]. The XRD data of the calculated grain size results obtained from X-ray diffraction experiments using the Scherrer formula calculated from the size of grain (D) is presented next shown in Eq. (1).

The equation is expressed as.

$$D = \frac{0.9\lambda}{\beta\cos\theta(rad)} \tag{1}$$

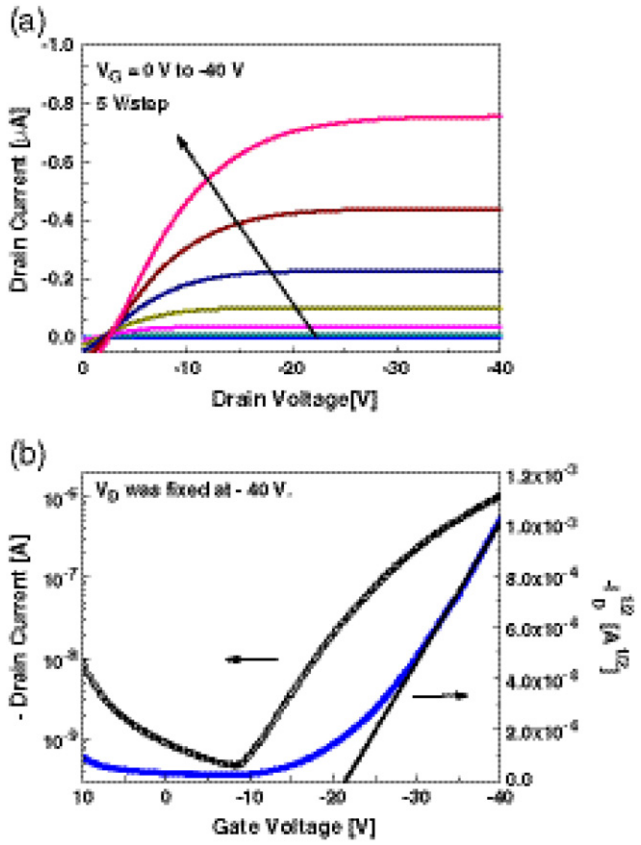

Fig. 4. Electrical properties of *p*-channel pentacene TFT (a) drain current–drain voltage (I_D–V_D) output curves, (b) transfer curves obtained at a drain bias of −40 V.

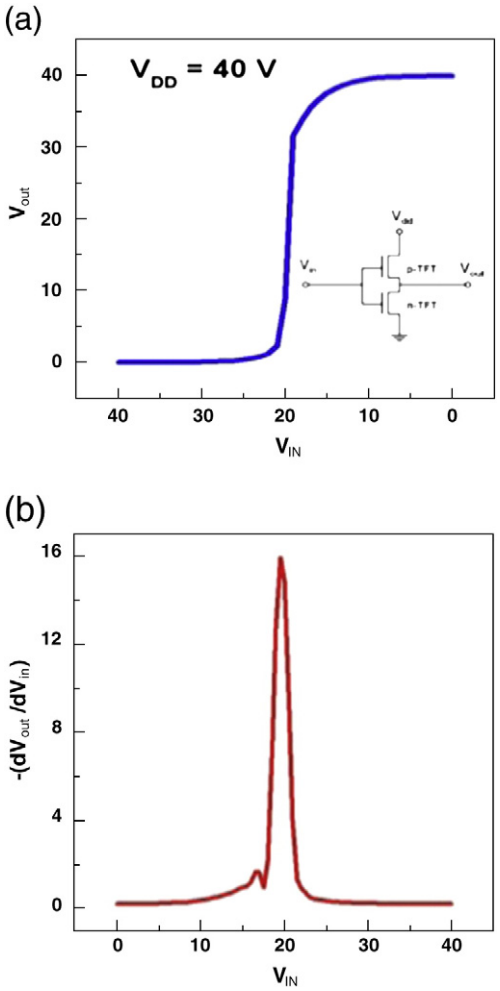

Fig. 5. Device performances of our hybrid CTFT inverter. (a) Static behavior of our inverter circuit composed of *p*-channel pentacene TFT and *n*-channel ZnO TFT, (b) operates well at a V_{DD} of 40 V with a high gain − (dV_{OUT}/dV_{IN}) of ~16 V.

where, *D* is the mean crystallite dimension, λ is the X-ray wavelength, typically 1.54 Å, β is the line broadening at half the maximum intensity (FWHM) in radians, and θ is the Bragg angle [25,26].

As calculated result, grain size of ZnO and pentacene are each 200 Å and 500 Å. Fig. 3(a) displays typical drain current–voltage (I_D–V_D) for a TFT with a ZnO active channel. Under a gate bias (V_G) of 40 V, a saturation current of more than 2.2 μA is achieved with full saturation at a drain bias of 40 V. Relatively, Fig. 4(a) shows I_D–V_D for a TFT with a pentacene active channel. Under a gate bias (V_G) of −40 V, although the current level of the pentacene TFT appeared slightly lower (~0.8 μA) than that of the ZnO TFT, our hybrid TFT pair was expected to operate well as a complementary device. Figs. 3(b) and 4(b) show the $\sqrt{I_D}$−V_G curves obtained at a drain bias of 40 V for the ZnO TFT and −40 V for the pentacene, respectively. For the OxTFT the estimated saturation μ_E is 1.3 $cm^2/V\,s$, V_T is 22 V and I_{ON-OFF} is 2.76×10^4, while for the OTFT μ_{FE} is 0.7 $cm^2/V\,s$, V_T is −21 V and I_{ON-OFF} is 1.26×104. This is fabricated and designed similar electronic property thought adjusting geometry of *n*-type TFT and *p*-type TFT. In the result, mobilities, I_{ON-OFF} and V_T of the ZnO and pentacene TFTs are similar. Fig. 5 shows the static behavior of proposed CTFT with the hybrid channels and the CTFT appears fully operational at a supply voltage (V_{DD}) of 40. The inverter response to stage switching is clearly observed between 0 and 40 V for input directions. Displaying a high maximum voltage gain − (dV_{OUT}/dV_{IN}) of ~16, as seen in Fig. 5(b). When the inverter is swept from 0 to 40 V via the input voltage, the pentacene channel itself experiences a substantial sweep from −40 to 0 V while the ZnO channel does so from 0 to 40 V. On the other hand, when the inverter is swept from 40 to 0 V, the two TFT go through the bias sweep in the opposite directions. It has been shown that, the performances of the proposed CTFT inverter are comparable, and even surpass those of previously reported complementary thin-film devices, in terms of voltage gain and driving voltage [27,28]].

4. Conclusion

In the experimental studies, firstly, each OTFT and OxTFT, is fabricated, and single devices are seen to have made similar characteristics even though they have different structures, and, using this result, the CTFT inverter has been fabricated. Secondly, if the hybrid inverter is fabricated using existing methods, the device, according to the channel type, can be fabricated using different S/D electrodes to achieve the required Ohmic contact is achieved the required Ohmic contact. However, the Ohmic contact is achieved with different channel types, using multi-layer Ti/Au electrodes of the same electrode fabricated through an adapted staggered structure for the *n*-type, and a coplanar structure for the *p*-type. As a result, etch single device fabricate Organic TFT and Inorganic TFT. In organic, p-type TFT device property of the adapted *p*-channel active — pentacene shows $M_{FE}=0.1\,[cm^2/V\,s]$, On–Off ratio $=1.26\times10^4$, $V_{TH}=-19$[V] and In inorganic, *n*-type TFT device of the adapted n channel active — ZnO shows $M_{FE}=0.03\,[cm^2/V\,s]$, On–Off ratio $=2.76\times10^4$, $V_{TH}=21$[V]. And hybrid inverter, the inverter response to stage switching was clearly observed between 0 and 40 V for both input directions, displaying a high maximum voltage gain − (dV_{OUT}/dV_{IN})>16.

Acknowledgment

This work was supported by the World Class University (WCU, R32-2008-000-10082-0) Project of the Ministry of Education, Science and

Technology (Korea Science and Engineering Foundation), the Basic Science Research Program through the National Research Foundation of Korea(NRF) funded by the Ministry of Education, Science and Technology (No.2009-0083126) and the IT R&D program of MKE/KEIT [KI002182, TFT backplane technology for next generation display].

References

[1] H. Sirringhaus, N. Tessler, R.H. Friend, Science 280 (1998) 1741.
[2] C.D. Dimitrakopoulos, S. Purushothaman, J. Kymissis, A. Callegari, J.M. Shaw, Science 283 (1999) 822.
[3] M. Halik, H. Klauk, U. Zschieschang, G. Schmid, C. Dehm, M. Schutz, S. Maisch, F. Effenberger, M. Brunnbauer, F. Stellacci, Nature (London) 431 (2004) 963.
[4] Elvira M.C. Fortunato, Pedro M.C. Barquinha, Ana C.M.G. Pimentel, Alexandra M.F. Goncalves, Antonio J.S. Marques, Rodrigo F.P. Martins, Luis M.N. Pereira, Appl. Phys. Lett. 85 (2004) 2541.
[5] E. Fortunato, P. Barquinha, A. Pimentel, A. Marques, L. Pereira, R. Martins, Thin Solid Film 487 (2005) 205.
[6] H. Klauk, M. Halik, U. Zschieschang, F. Eder, D. Rohde, G. Schmid, C. Dehm, IEEE Trans. Electron Devices 52 (2005) 618.
[7] S.D. Vusser, S. Steudel, K. Myny, J. Genoe, P. Heremans, Appl. Phys. Lett. 88 (2006) 162116.
[8] M.H. Yoon, H. Yan, A. Facchetti, T.J. Marks, J. Am. Chem. Soc. 127 (2005) 10388.
[9] R.L. Hoffman, J. Appl. Phys. 95 (2004) 5813.
[10] Yoichi Ogo, Hidenori Hiramatsu, Kenji Nomura, Hiroshi Yanagi, Toshio Kamiya, Masahiro Hirano, Hideo Hosono, Appl. Phys. Lett. 93 (2008) 032113.
[11] H. Hosono, N. Kikuchi, N. Ueda, H. Kawazoe, J. Non-Cryst. Solids 198 (1996) 165.
[12] C.D. Dimitrakopoulos, P.R.L. Malenfant, Adv. Mater. (Weinheim,Ger.) 14 (2002) 99.
[13] C.R. Kagan, P. Andry, Thin-Film Transistors (Dekker, New York) (2003) 325.
[14] W.J. Kim, W.H. Koo, S.J. Jo, C.S. Kim, H.K. Baik, J. Lee, S. Im, Electrochem. Solid-State Lett 8 (2005) G341.
[15] Ch. Pannemann, T. Diekmann, U. Hilleringmann, J. Mater. Res. 19 (2004) 1999.
[16] Min Suk Oh, D.K. Hwang, Kimoon Lee, Won Jun Choi, Jae Hoon Kim, Seongil Im, J. Appl. Phys. 102 (2007) 076104.
[17] Jeong- M. Choi, Jae Hoon Kim, Seongil Im, Appl. Phys. Lett. 91 (2007) 083504.
[18] Kazuki Hizu, Tsuyoshi Sekitani, Takao Someya, Appl. Phys. Lett. 90 (2007) 093504.
[19] Kimoon Lee, Ki-tae Kim, Kwang H. Lee, Gyubaek Lee, Min Suk Oh, Jeong-M. Choi, Seongil Im, Sungjin Jang, Eugene Kim, Appl. Phys. Lett 93 (2008) 193514.
[20] C.R. Kagan, A. Afzali, T.O. Graham, Appl. Phys. Lett. 86 (2005) 193505.
[21] Oh. Byeong-Yun, Min-Chang Jeong, Moon-Ho Ham, Jae-Min Myoung, Semicond. Sci. Technol. 22 (2007) 608.
[22] E.M. Suuberg, J. Chem, Eng. Data 43 (1998) 486–492.
[23] Ricardo Ruiz, Devashish Choudhary, Bert Nickel, Tullio Toccoli, Kee-Chul Chang, Alex C. Mayer, Paulette Clancy, Jack M. Blakely, Randall L. Headrick, Salvatore Iannotta, George G. Malliaras, Chem. Mater. 16 (2004) 4497.
[24] Frederik Claeyssens, Colin L. Freeman, Neil L. Allan, Ye. Sun, Michael N.R. Ashfold, John H. Harding, J. Mater. Chem. 15 (2005) 139.
[25] P. Scherrer, Göttinger Nachrichten Gesell 2 (1918) 98.
[26] A.L. Patterson, Phys. Rev. 56 (10) (1939) 978.
[27] Carl.R. Nave, Bragg's Law, HyperPhysics, Georgia State University, 2008 // hyperphysics.phy-astr.gsu.edu/hbase/quantum/bragg.html, retrieved.
[28] H. Klauk, M. Halik, U. Zschieschang, F. Eder, D. Rohde, G. Schmid, C. Dehm, IEEE Trans Electron Devices 52 (2005) 618.